

PAPER

Inscription of surface waveguides in glass by femtosecond laser writing for enhanced evanescent wave overlap

To cite this article: Vitor A Amorim *et al* 2020 *J. Opt.* **22** 085801

View the [article online](#) for updates and enhancements.

You may also like

- [Multi-photon high-excitation-energy approach to fibre grating inscription](#)
David N Nikogosyan
- [Wavelength-switchable erbium-doped fiber laser based on femtosecond FBG inscribed on fiber core and cladding through the coating](#)
Wei He, Guoshun Zhong, Lianqing Zhu et al.
- [Bragg grating-based Fabry–Perot interferometer fabricated in a polymer fiber for sensing with improved resolution](#)
G Statkiewicz-Barabach, P Mergo and W Urbanczyk

Inscription of surface waveguides in glass by femtosecond laser writing for enhanced evanescent wave overlap

Vítor A Amorim^{1,2} , João M Maia^{1,2} , Duarte Viveiros^{1,2} and P V S Marques^{1,2}

¹ Centre for Applied Photonics, INESC TEC, Porto 4150-179, Portugal

² Department of Physics and Astronomy, University of Porto, Porto 4169-007, Portugal

E-mail: viktor.a.amorim@inesctec.pt

Received 27 March 2020, revised 10 June 2020

Accepted for publication 25 June 2020

Published 9 July 2020



CrossMark

Abstract

Near-surface optical waveguides were fabricated in alkaline earth boro-aluminosilicate glass (Eagle2000), by femtosecond laser direct writing, using two distinct approaches. First, the capability of directly inscribing optical waveguides close to the surface was tested, and then, compared to the adoption of post writing wet etching to bring to the surface waveguides inscribed at greater depths. Laser ablation was found to limit the minimum surface to core center distance to $6.5\ \mu\text{m}$ in the first method, with anisotropic wet etching limiting the latter to $3\ \mu\text{m}$ without any surface deformation; smaller separations can be achieved at the cost of the planar surface topography. Furthermore, the waveguide's cross-section was seen to vary for laser inscription nearing the surface, observations that were also corroborated by its distinct guiding characteristics when compared to the adoption of post writing wet etching. The spectral analysis (in the 500–1700 nm range) also evidenced an increase in insertion loss for longer wavelengths and smaller surface to core center separations, caused, most likely, by coupling loss due to the interaction between the propagating mode and the surface. Different lengths of waveguide exposed to the surface were also tested, revealing that scattering loss due to surface roughness is not an issue at the centimeter scale.

Keywords: femtosecond laser direct writing, surface waveguides, wet etching

(Some figures may appear in colour only in the online journal)

1. Introduction

The inscription of optical waveguides in glass using a femtosecond laser was first demonstrated by Davis *et al* in 1996 [1]. Since then, this technique has emerged as an impressive complementary tool with the capability of producing three-dimensional photonic devices in transparent dielectric materials, differentiating itself from the traditional two-dimensional photolithographic methods. Furthermore, it does not require masks or multiple fabrication steps, offering prototyping flexibility. Even though it is a serial process, which translates into a lack of scalability, and, thus, a low throughput, some materials allow very high scan velocities [2], severely reducing fabrication times.

The development of optical sensors has accelerated in the last few decades, with optical fibers contributing immensely in

this growth. Due to the extremely low loss achieved nowadays, optical fibers provide an almost ideal optical platform for the development of such applications. Usually, optical fiber sensors are based on the interaction between the evanescent wave and the outer medium. As such, the removal of part of the cladding [3] or tapering [4] is commonly employed, increasing the fragility of the already delicate optical fibers. Femtosecond laser direct writing can circumvent this issue, as the optical platforms can be developed in bulk, and thus sturdy, glass substrates. In this case, the evanescent wave can be exposed by the inscription of waveguides nearing the surface of the substrates, with some works having already studied this possibility [5–7]. Other works have also used this approach in the fabrication of optical sensors, such as: intensity-based refractive index sensors [7, 8], surface plasmon resonance-based refractive index sensors [9], detectors

for the water's phase as well as the type of ice microstructure [10], and whispery gallery mode excitation platforms that may be used in optical sensing [11]. However, some difficulties in producing such platforms still exist. This is mainly due to the limit set by ablation at the surface, forcefully increasing the separation between the surface and the waveguide's core center, and the limitations imposed by the methods trying to avoid such issue. Also, the present studies still lack an exhaustive characterization of the waveguides' dependence on inscription depth as well as the evolution of their broadband spectral response.

In this work, we report a thorough study on the fabrication of near-surface waveguides embedded in Eagle2000 using femtosecond laser direct writing. Two distinct manufacturing methods were compared, with the influence of the surface to core center distance in the structures' cross-section and spectral response being analyzed. Different surface interaction lengths were tested, and the effect of surface roughness on propagation loss evaluated.

2. Experimental procedure

In this work, a fiber amplified femtosecond laser (Satsuma HP, Amplitude Systèmes)—operating at 515 nm, with a pulse duration of approximately 250 fs and a repetition rate of 1 MHz—was used to inscribe optical waveguides in alkali-free borosilicate glass (Eagle2000). Coupled to the laser was a Workshop of Photonics workstation equipped with Aerotech direct-drive stages (ANT130XY-110 PLUS and ANT130 V-5 PLUS). These were used to scan the substrate transversely to the linearly polarized beam, which was focused into the substrate via a 0.42 numerical aperture plan apochromat objective (Mitutoyo M Plan Apo NIR 50x). The scan direction was maintained throughout the inscription process in order to avoid the Quill effect [12], with the beam polarization being set parallel to the writing direction.

Wet etching, when employed, was made using a solution composed by HF 1%/HCl 37% 10/2 (V/V). Initially, an HF acid solution was tested, however, a large surface roughness was observed. As in [13], this was the result of the deposition of insoluble products on the substrate's surface, creating masking layers that prevent a uniform removal of the material; the insoluble products originated from oxides in the glass structure become soluble in the presence of HCl acid in the solution. Thus, the etchant solution was optimized for Eagle2000 and the results are depicted in figure 1 for future reference.

In order to obtain a defect-free waveguide cross-section, the side facets of all substrates were polished before characterization. This damage derives primarily from the laser beam crossing the air/glass boundary and from the etching process due to etching selectivity. To characterize the waveguides' spectral response, a broadband source was coupled to a single-mode fiber (SMF-28) which was then butt-coupled to the entrance facet of the near-surface waveguides. The substrates and the input/output optical fibers were fixated on an Elliot Martock MDE881 stage, which is equipped with piezo controls (Dali E-2100) for precise alignment. Light exiting from

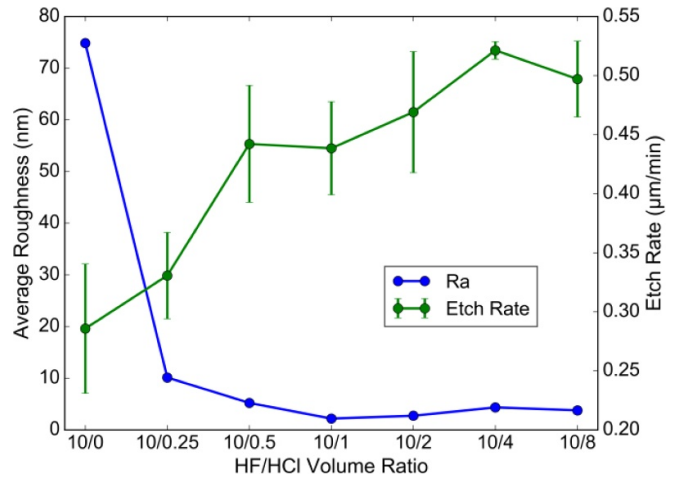


Figure 1. Average surface roughness, R_a , and etch rate for different HF (1%) to HCl (37%) volumetric ratios; the etch reaction extended for 80 min at a temperature of 40°C in an ultrasonic bath (Branson 2510). Roughness measurements were made using a profilometer (Dektak XT, Bruker) with a stylus radius of 2 μm .

the inscribed optical waveguides is collected and guided by a second butt-coupled optical fiber to an optical spectrum analyzer (ANDO AQ-6315B), where it is inspected from 500 nm to 1700 nm with a 10 nm resolution. For normalization purposes, the broadband source's spectrum was recorded prior to any measurements. To minimize Fresnel reflections at the input/output fibers/facets, index matching (Cargille series: AA $n_D^{25^\circ\text{C}} = 1.4580 \pm 0.0002$) was used.

3. Experimental results and discussion

In this study, several 24 mm long near-surface modification tracks were fabricated in Eagle2000 while varying inscription depth in steps of 0.5 μm . For this, a fixed pulse energy of 125 nJ and a scan velocity of 6 cm s^{-1} was used. This choice of parameters is substantiated in a previous work of ours [2], as it was shown to yield low-loss optical waveguides over a 1200 nm range (from 500 to 1700 nm) with a relatively small cross-section. Furthermore, such parameters yield an optical waveguide nearing the cut-off at longer wavelengths, resulting in a structure whose modes supported are larger. This characteristic is of relevance, as it influences the overlap of the propagating mode with the dielectric medium outside of the substrate's surface, thereby improving the performance of future sensing devices.

Figure 2(a) displays a schematic of the straight near-surface modification tracks that were inscribed at different depths, with figure 3 displaying their cross-section. In figure 3 (top), the inscription depth is represented at the top left of the image of each scan, with 0 μm corresponding to the writing beam focused at the surface, and further values showing the increase in inscription depth. As can be seen, the type of photo-induced modification [14] is highly dependent on depth (in the range tested). The threshold for the formation of type III modifications increases as the beam focus is moved farther from

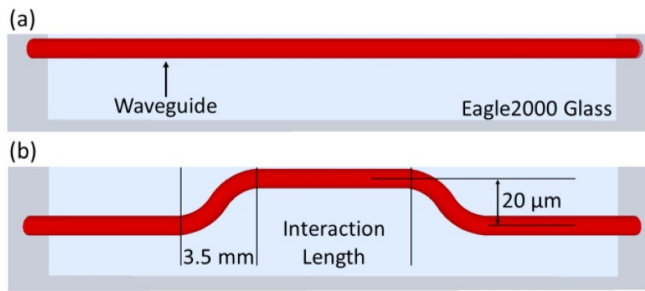


Figure 2. Schematic of the devices fabricated and studied in this work. (a) The inscription of straight near-surface waveguides, and (b) the design used for testing different surface interaction lengths.

the substrate's surface, evidenced by the replacement of surface ablation (type III) for a structure with an isotropic index change (type I). We can also see that this replacement is not immediate, requiring a depth of approximately $16\ \mu\text{m}$ to completely transition to a type I modification. This value is not fixed, with a lower pulse energy and higher scan velocity being able to further reduce it, although a significant loss in waveguiding capabilities at longer wavelengths is to be expected [2]. Early type I structures are also very different of those fabricated at greater depths, namely in their dimensions and refractive index modification, with most of the variability being found near the surface. This translates into waveguiding structures with distinct intrinsic guiding properties that only stabilize when fabricated at greater depths. Therefore, the minimum distance achieved between the center of the core of a, mostly, stable waveguide and the surface was $6.5\ \mu\text{m}$ (represented by an inscription depth of $17\ \mu\text{m}$), limiting the overlap of the propagating mode's evanescent field with the dielectric medium at the substrate's surface. These results are in accordance with previous works made in the same material [6, 15], where inscription at shallow depths resulted in ablation. Other studies in Gorilla glass have shown mixed results in this aspect, with some reporting near-surface waveguides being achievable [5, 6], while others found a minimum surface to core center separation of $25\ \mu\text{m}$ [11].

Alternative ways of mitigating ablation were reported; for instance, the use of van der Waals forces established between a cover slide and a substrate to suppress the air-glass interface [6], or by using silver-containing zinc phosphate glass, where the refractive index change is achieved by triggering the photochemistry of silver without affecting the glass structure [7]. However, these methods present limitations in its fabrication and/or mass production capabilities, namely: (1) the use of a cover slide to suppress the air-glass interface requires both surfaces to be extremely clean, as to guarantee the quality of the contact; defects will result in localized ablation. Furthermore, the top of the waveguides inscribed are limited to the substrate's surface, since an inscription between both interfaces results in laser welding [16]. (2) Laser inscription in silver-containing zinc phosphate glass requires very small scan velocities in the order of $50\ \mu\text{m}\ \text{s}^{-1}$ [7], drastically increasing the fabrication times of such devices.

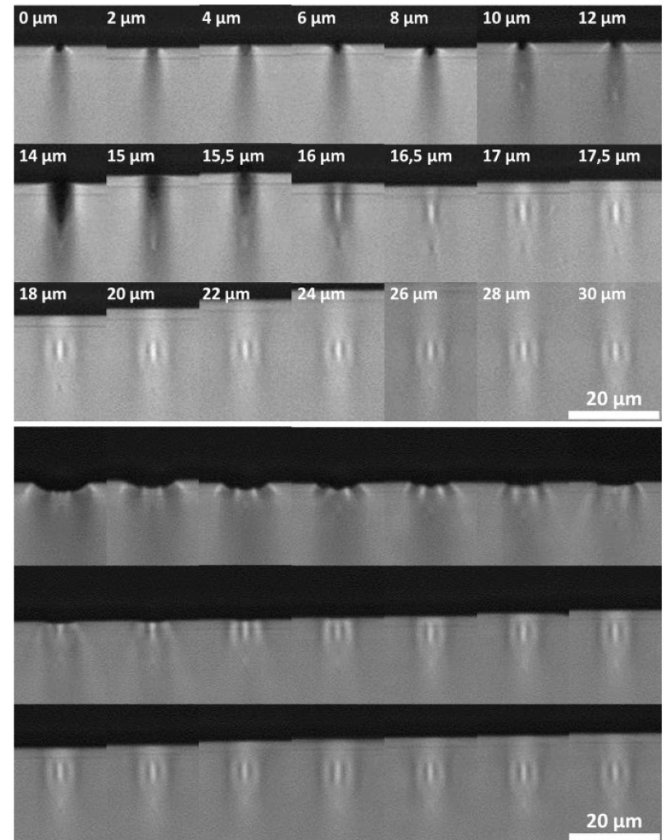


Figure 3. Transmission mode optical microscope images of the cross-section of modification tracks produced in Eagle2000 at various depths without any surface modification (top) and with wet etching (bottom). (Top) depicts an inscription process starting at the substrate's surface up to a depth of $30\ \mu\text{m}$, while (bottom) displays the result of translating optical waveguides—inscribed with an initial surface to core center distance between 20 and $30\ \mu\text{m}$, increasing in steps of $0.5\ \mu\text{m}$ —to the surface using wet etching. A pulse energy of $125\ \text{nJ}$ and a scan velocity of $6\ \text{cm}\ \text{s}^{-1}$ were used in all scans. Laser inscription was made from the top to the bottom.

In this work, we propose the adoption of post writing wet etching in order to achieve superficial optical waveguides whose surface to core center distance can be tuned beyond the limitations imposed by ablation. Figure 3 (bottom) depicts the result of fabricating optical waveguides at different depths, followed by a single wet etching process with HF (1%)/HCl (37%) 10:2 (V/V); an initial surface to core center distance of $20\ \mu\text{m}$ was used, with the inscription depth of the following waveguides increasing in steps of $0.5\ \mu\text{m}$, thus ensuring a stable type I modification. As illustrated, this method allows the translation of optical waveguides fabricated at greater depths up to the surface while conserving their features. Due to the presence of etch selectivity, optical waveguides whose top has come into contact with the surface are partially etched, with the amount of material removed depending on the time that the waveguide has been exposed, as depicted in the first waveguides of figure 3 (bottom). This translates into a minimum surface to core center separation of $3\ \mu\text{m}$ without any signs of etch anisotropy, with smaller separations

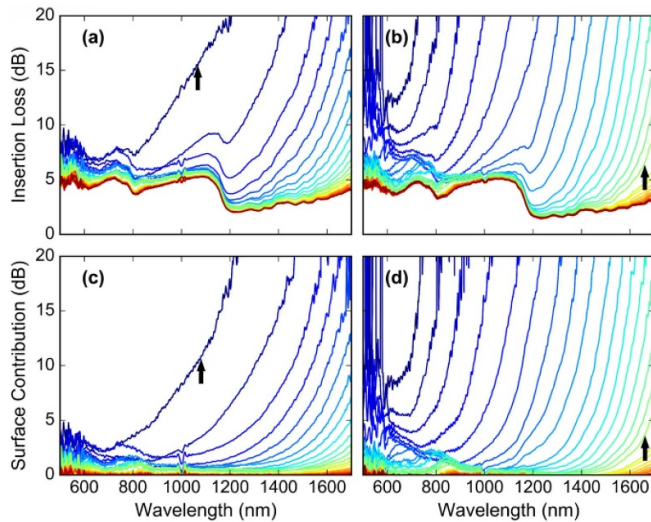


Figure 4. Insertion loss (a), (b) and loss due to the surface contribution (c), (d) of 24 mm long optical waveguides as a function of wavelength for different inscription depths. Surface contribution was calculated by the subtraction of all insertion loss spectra with that of a waveguide fabricated at a depth of $100\ \mu\text{m}$. The spectra represented in (a), (c) correspond to waveguides displayed in figure 3 (top), while the spectra in (b), (d) correspond to waveguides displayed in figure 3 (bottom). Dark blue represents the shallowest waveguide, transitioning to red as depth increases in steps of $0.5\ \mu\text{m}$. The shallowest waveguide in (a), (c) is represented in figure 3 (top) for an inscription depth of $17\ \mu\text{m}$, while the shallowest waveguide in (b), (d) is represented in the top left of figure 3 (bottom). Waveguides with a surface to core center distance of approximately $6.5\ \mu\text{m}$ are identified by arrows.

being achievable at the expense of increasing surface modification. It should be noted, however, that the minimum separation distance mentioned is not fixed and will vary upon the change of fabrication parameters; waveguides fabricated at higher pulse energies and/or lower scan velocity will see this minimum separation increase and vice-versa due to the variation in the dimensions of the modification.

Thus, this method enables the production of both buried and on-surface waveguides, while also allowing the fine-tuning of the surface to core center distance. In principle, the same can be achieved through mechanical polishing, although it was not used here due to the simplicity of wet etching. There are, however, advantages to mechanical polishing, such as the inexistence of selectivity in the removal of material, allowing the development of optical waveguides at any separation while maintaining the surface's topography.

The spectral characteristics of the optical waveguides depicted in figure 3 were also analyzed, as can be seen in figure 4; waveguides displayed in figure 3 (top) are represented in figures 4(a) and (c), while the waveguides displayed in figure 3 (bottom) are represented in figures 4(b) and (d). In both cases, the spectrum of the shallowest waveguide is represented in dark blue, with depth increasing in steps of $0.5\ \mu\text{m}$ as color transitions to red. The shallowest waveguide in figures 4(a) and (c) is represented in figure 3 (top) for an inscription depth of $17\ \mu\text{m}$, while in figures 4(b) and (d) the shallowest waveguide is represented at the top left of figure 3 (bottom). As can be

observed, the losses increase monotonically with wavelength. This behavior was already observed in other works [2, 17], and corresponds to a decrease in V-number due to an increase in wavelength, causing larger coupling losses. Furthermore, this monotonic growth steepens as depth decreases, indicating greater coupling losses as the waveguides near the surface. It is known that larger coupling losses result from the mismatch between two propagating modes; in this case between the waveguide's mode and the one supported by the input/output butt-coupled fibers. Usually, in the fabrication of waveguides, the variation in coupling loss is intimately related with the writing parameters, since these affect the refractive index and dimensions of the modification. Here, however, the parameters were fixed, meaning that any change in coupling loss should be related with the surface. As discussed previously, the characteristics of near-surface optical waveguides fabricated without wet etching, such as those displayed in figure 3 (top), only stabilize at greater depths. Thus, an alteration in the propagated mode's diameter is to be expected, explaining part of the increase in loss. The other part has to do with the influence of the dielectric medium outside the substrate, which in this case is air. As the waveguide approaches the surface, its propagating mode is distorted due to the refractive index contrast at the boundary, adding to the loss mentioned above. In the case of waveguides fabricated at greater depths and then etched to the surface, as in figure 3 (bottom), the reasoning is very similar. Again, part of the loss observed is due to the refractive index contrast at the boundary that deforms the propagating mode. The rest is, in this case, explained by the removal of material of the waveguide, resulting in its smaller dimensions and, hence, smaller V-number, which will ultimately result in additional coupling loss. We also conclude that the insertion loss of two near-surface waveguides fabricated with and without wet etching, while maintaining the same writing parameters and surface to core center distance, is different. This is most obvious when comparing the shallowest waveguide achieved without wet etching with one produced after wet etching at a surface to core center distance of $6.5\ \mu\text{m}$ (represented by arrows in figures 4 (a), (c) and (b), (d), respectively). In the latter case, the losses are severely reduced even though all fabrication parameters are the same; as was already mentioned, this has to do with the effect that the surface has on the dimensions and refractive index of the waveguide, with these effects being lessened as inscription depth increases. Hence, if one requires that the waveguides' physical properties remain constant, inscription at slightly greater depths followed by wet etching, or even mechanical polishing, should be employed.

The dependence of the spectral characteristics on the length of the near surface waveguides was also studied, as can be seen in figure 5. For this, several waveguides were fabricated at different depths in steps of $0.5\ \mu\text{m}$, and then etched to the surface as before. This time, however, instead of inscribing straight waveguides at a constant depth, the waveguides were inscribed with $3.5\ \text{mm}$ long vertical S-bends that shift the propagating mode(s) $20\ \mu\text{m}$ closer to the surface, as in figure 2(b). This geometry makes more sense in real life applications, as the waveguide's end facets are more protected from the fragile edges, and because the interaction length (length

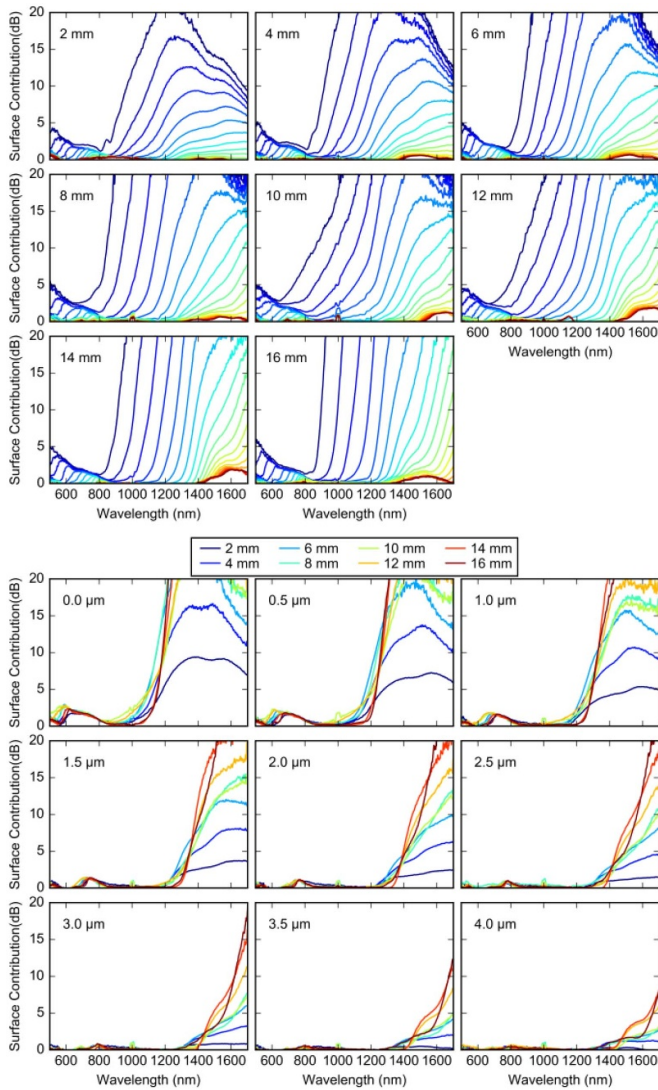


Figure 5. Surface's contribution to loss as a function of wavelength for: varying depth in the range of interaction lengths tested (top) and varying interaction length for a surface to core center distance between 0 and 4 μm (bottom). (Top) The spectrum of the shallowest waveguide in each case is represented in dark blue, with depth increasing in steps of 0.5 μm as color transitions to red.

of the waveguide exposed to the surface) can be easily tuned to accommodate the desired application without being limited to the substrate's dimensions. From figure 5 (top), we can observe the surface's contribution to insertion loss for several surface to core center separations plotted for the different interaction lengths tested, while in figure 5 (bottom) the same is represented for the various interaction lengths tested plotted for a surface to core center separation between 0 and 4 μm . Intuitively, one would think that a greater interaction length results in greater insertion loss, particularly due to propagation loss originated from scattering at the surface. Thus, an almost wavelength-independent increase in baseline loss and/or a C/λ^4 trend created by Mie and/or Rayleigh scattering, respectively, should be visible. However, that is not

the case, indicating that the surface roughness is not an issue at this scale. Instead, some features are detected, namely: (1) the existence of a small peak between 500 and 800 nm that redshifts when the surface to core center distance increases, maintaining its behavior across all interaction lengths, (2) the additional loss found at longer wavelengths for increasing interaction length, keeping the spectral characteristics of such waveguides from matching those of straight optical waveguides, and (3) the fact that the loss at longer interaction lengths drops monotonically, as wavelength increases, when the interaction length and surface to core center decreases—best observed in figure 5 (top) for an interaction length of 2 mm at wavelengths greater than 1200 nm. Firstly, the small peak between 500 and 800 nm is most likely due to coupling loss induced by a second propagated mode. There are two clues to this reasoning. The presence of a significant blue shift when the surface to core center distance decreases—and, more specifically, when the waveguides' dimensions diminish due to material removal—is indicative of a reduction in the cut-off wavelength. Also, the lack of dependence with interaction length indicates that propagation loss is not responsible for their origin. Secondly, the existence of additional loss at longer wavelengths, for increasing interaction length, is not compatible with a model based on coupling loss or scattering loss caused by either Rayleigh and/or Mie scattering; coupling loss should yield a behavior that is independent of interaction length, while scattering loss should result in a C/λ^4 trend and/or an almost wavelength-independent increase in baseline loss. Radiation loss caused by the S-bends' curvature is most likely the culprit here, with similar results being observed in optical fibers [18]. In this case, waveguides fabricated with a shorter interaction length, and thus a smaller separation between straight waveguides, display lower losses due to better light recoupling; longer interaction lengths translate into a larger separation between straight waveguides, leading to a poor light recoupling. Thirdly, the monotonic drop in loss at longer wavelengths, when the interaction length and surface to core center decreases, is also related to the bending loss discussed previously. In this circumstance, however, the coupling loss at longer wavelengths becomes so apparent that the increase in recoupled light, as wavelength increases, becomes noticeable.

4. Conclusions

The fabrication of near-surface optical waveguides, inscribed in alkaline earth boro-aluminosilicate glass substrates (Eagle2000) by femtosecond laser direct writing, was studied and their spectral response characterized. It was observed that, near the surface, the type of photo-induced modification is highly dependent on depth, with ablation occurring until it is replaced by a type I modification. Therefore, the minimum surface to core center distance achieved was limited to 6.5 μm . Also, a slight variation in the waveguide's cross-section was noticeable for different depths, with most

of the variability being found near the surface. This characteristic was corrected with the adoption of post writing wet etching, allowing the fabrication of waveguides at greater depths (where its cross-section has stabilized), and, then, their translation to the surface. In this case, the presence of etch selectivity limited the minimum surface to core center distance to 3 μm without any signs of etch anisotropy, with smaller separations being achievable together with increasing surface modification. Mechanical polishing could, in principle, allow the manufacturing of optical waveguides at any separation while maintaining the surface's topography. The insertion loss of two near-surface waveguides at the same surface to core center separation was also seen to differ in both approaches, which is most likely caused by the variability of the cross-section discussed above. Furthermore, the waveguides were seen to approach the cut-off as the surface to core center distance decreased, somewhat limiting their applicability due to larger coupling losses at longer wavelengths; such a feature can be minimized with a stronger modification. Also, propagation loss originated from scattering at the surface was not observable, indicating that the surface's roughness is not an issue at this scale.

Acknowledgments

This work was supported by Fundação para a Ciência e a Tecnologia through Grant No. SFRH/BD/128795/2017 and by Project 'On Chip Whispering Gallery Mode Optical Microcavities For Emerging Microcontaminant Determination In Waters' - SAFE WATER, which is supported and co-funded by the European Commission, Directorate-General Communications Networks, Content and Technology (DG CONNECT) under the ERA-NET Cofund scheme - Horizon 2020 'Horizon 2020—the Framework Programme for Research and Innovation (2014-2020)'.

ORCID iDs

Vítor A Amorim  <https://orcid.org/0000-0002-2173-2441>

João M Maia  <https://orcid.org/0000-0001-9260-4247>

References

- [1] Davis K M, Miura K, Sugimoto N and Hirao K 1996 *Opt. Lett.* **21** 1729–31
- [2] Amorim V A, Viveiros D, Maia J M and Marques P V S 2019 *IEEE Photon. Technol. Lett.* **31** 1658–61
- [3] Coelho L, Almeida J M M M, Santos J L, Ferreira R A S, André P S and Viegas D 2015 *Plasmonics* **10** 319–27
- [4] Tian Y, Wang W, Wu N, Zou X and Wang X 2011 *Sensors* **11** 3780–90
- [5] Lapointe J, Gagné M, Li M and Kashyap R 2014 *Opt. Express* **22** 15473–83
- [6] Bérubé J and Vallée R 2016 *Opt. Lett.* **41** 3074–7
- [7] Khalil A A, Lalanne P, Bérubé J, Petit Y, Vallée R and Canioni L 2019 *Opt. Express* **27** 31130–43
- [8] Lapointe J, Parent F, Filho E S L, Loranger S and Kashyap R 2015 *Opt. Lett.* **40** 5654–7
- [9] Zhang Y, Liao C, Lin C, Shao Y, Wang Y and Wang Y 2019 *Opt. Lett.* **44** 2434–7
- [10] Martínez J et al 2017 *Adv. Mater. Technol.* **2** 1700085
- [11] Çirkinoglu H O, Bayer M M, Gokay U S, Serpengüzel A, Sotillo B, Bharadwaj V, Ramponi R and Eaton S M 2018 *Appl. Opt.* **57** 3687–92
- [12] Kazansky P G, Yang W, Bricchi E, Bovatsek J, Arai A, Shimotsuma Y, Miura K and Hirao K 2007 *Appl. Phys. Lett.* **90** 151120
- [13] Iliescu C, Jing J, Tay F E H, Miao J and Sun T 2005 *Surf. Coat. Technol.* **198** 314–8
- [14] Poumellec B, Lancry M, Chahid-Er-raji A and Kazansky P G 2011 *Opt. Mater. Express* **1** 766–82
- [15] Zraggen E, Scholder O, Bona G, Fontana F, Alberti E, Crespi A, Osellame R, Scharf T and Shorubalko I 2015 *J. Opt.* **17** 025801
- [16] Richter S, Nolte S and Tunnermann A 2012 *Phys. Procedia* **39** 556–62
- [17] Amorim V A, Maia J M, Viveiros D and Marques P V S 2019 *J. Lightwave Technol.* **37** 2240–4
- [18] Faustini L and Martini G 1997 *J. Lightwave Technol.* **15** 671–9